

1 **Fine-tuning heat stress algorithms to optimise global predictions of mass coral bleaching**

2 *Liam Lachs^{1,*}, John C. Bythell¹, Holly K. East², Alastair J. Edwards¹, Peter J. Mumby^{4,5}, William J.*
3 *Skirving^{6,7}, Blake L. Spady^{6,7}, James R. Guest¹*

4 ¹School of Natural & Environmental Sciences, Newcastle University, Newcastle upon Tyne, NE1 7RU, UK

5 ²Department of Geography and Environmental Sciences, Northumbria University, Newcastle upon Tyne, UK

6 ⁴Marine Spatial Ecology Lab, School of Biological Sciences, University of Queensland, St Lucia, Queensland
7 4072, Australia

8 ⁵Palau International Coral Reef Center, Koror, Palau

9 ⁶Coral Reef Watch, National Oceanic and Atmospheric Administration, College Park, MD 20740, USA

10 ⁷ReefSense Pty, Ltd., P.O. Box 343, Aitkenvale BC, Aitkenvale, QLD 4814, Australia

11 *Corresponding Author:

12 Liam Lachs – l.lachs2@newcastle.ac.uk

13 **Abstract**

14 Increasingly severe marine heatwaves under climate change threaten the persistence of many marine
15 ecosystems. Mass coral bleaching events, caused by periods of anomalously warm sea surface
16 temperatures (SST), have led to catastrophic levels of coral mortality globally. Remotely monitoring
17 and forecasting such biotic responses to heat stress is key for effective marine ecosystem
18 management. The Degree Heating Week (DHW) metric, designed to monitor coral bleaching risk,
19 reflects the duration and intensity of heat stress events, and is computed by accumulating SST
20 anomalies (HotSpot) relative to a stress threshold over a 12-week moving window. Despite significant
21 improvements in the underlying SST datasets, corresponding revisions of the HotSpot threshold and
22 accumulation window are still lacking. Here, we fine-tune the operational DHW algorithm to optimise
23 coral bleaching predictions using the 5km satellite-based SSTs (CoralTemp v3.1) and a global coral
24 bleaching dataset (37,871 observations, National Oceanic and Atmospheric Administration). After
25 developing 234 test DHW algorithms with different combinations of HotSpot threshold and
26 accumulation window, we compared their bleaching-prediction ability using spatiotemporal Bayesian
27 hierarchical models and sensitivity-specificity analyses. Peak DHW performance was reached using
28 HotSpot thresholds less than or equal to Maximum Monthly Mean SST and accumulation windows of
29 4 – 8 weeks. This new configuration correctly predicted up to an additional 310 bleaching
30 observations compared to the operational DHW algorithm, an improved hit rate of 7.9 %. Given the
31 detrimental impacts of marine heatwaves across ecosystems, heat stress algorithms could also be fine-
32 tuned for other biological systems, improving scientific accuracy, and enabling ecosystem
33 governance.

34 **Keywords**

35 spatiotemporal Bayesian modelling; R-INLA; remote sensing; marine heatwaves; coral bleaching

36 **Introduction**

37 Anthropocene marine heatwaves are becoming increasingly intense, more frequent and longer lasting
38 due to climate change (Oliver et al. 2018; Holbrook et al. 2019). These anomalous heat stress events
39 can have severe implications for a range of marine biota, e.g., influencing shifts in zooplankton
40 communities, declines in key groups such as krill (Jiménez-Quiroz et al. 2019; Evans et al. 2020;
41 Işkın et al. 2020), die-offs and reproductive failures of sea-birds (Cavole et al. 2016; Jones et al. 2018;
42 Piatt et al. 2020), marine mammal strandings (Cavole et al. 2016), and mass coral bleaching and
43 mortality events (Hughes et al. 2018). While surveying in situ ecosystem responses to climate change
44 disturbances are essential to assess impact, it is also very costly. Accurate monitoring of ecosystem

45 stress remotely and at scale is therefore crucial for effectively managing marine ecosystems and
46 accurately predicting the impacts of climate change on marine biota. While satellite-based remote
47 monitoring and forecasting programmes have been implemented across various biological contexts,
48 we focus this study specifically on remote monitoring and forecasting of coral bleaching. Coral reefs
49 are highly productive ecosystems that provide habitat to over a million marine species and essential
50 ecosystem services (e.g., coastal protection, food, fisheries and tourism livelihoods) to hundreds of
51 millions of people, estimated to be worth over 350,000 USD/ha/yr globally (Costanza et al. 2014;
52 Ferrario et al. 2014). These ecosystems are increasingly faced with mass coral bleaching and mortality
53 events (Hughes et al. 2017). The process of coral bleaching involves a breakdown in the symbiosis
54 between coral hosts and their endosymbiotic phototrophic algae, and can ultimately lead to full or
55 partial colony mortality (Brown 1997) and sub-lethal effects such as reduced growth (Edmunds 2005).
56 Coral bleaching is a stress response with a variety of triggers (e.g., 2003 anomalous temperature, both
57 high and low; anomalous increases in the level of light; anomalous levels of salinity, both high and
58 low; reduction in water quality; and diseases; Skirving et al. 2018). Episodes of mass coral bleaching
59 occur across large spatial scales, affect numerous coral taxa, and can destroy entire healthy reefs
60 within months. Pantropical mass bleaching events are becoming recurrent and are caused by the
61 widespread increasing incidence of marine heatwaves under climate change (Hughes et al. 2017;
62 Donner et al. 2018; Hoegh-Guldberg et al. 2019).

63 Over the past two decades, the National Oceanic and Atmospheric Administration's (NOAA) Coral
64 Reef Watch (CRW) programme has developed a suite of tools for monitoring coral bleaching risk
65 using satellite-based sea surface temperature (SST) products. Specifically, the Degree Heating Week
66 (DHW) metric is used as an indicator of heat stress levels sufficient to induce coral bleaching. DHW
67 is computed as the accumulation of positive temperature anomalies (HotSpot) above a hypothesised
68 coral bleaching stress temperature (i.e., 1°C above the Maximum of Monthly Means SST climatology
69 – MMM) over the previous 12 weeks (Liu et al. 2003; Skirving et al. 2020). The DHW algorithm was
70 designed in the 1990s, and the HotSpot threshold of 1°C above MMM and accumulation window of 12
71 weeks were chosen based on field and experimental evidence from Panama and the Caribbean (Glynn
72 and D'Croz 1990; Jokiel and Coles 1990). Reflecting the technological advancements in remote-
73 sensing capabilities since then, the SST and DHW products have increased in spatial resolution (50
74 km to 5 km) and temporal resolution (twice weekly to daily) (Liu et al. 2014). Despite these
75 improvements, there has not yet been a corresponding revision of the HotSpot threshold and
76 accumulation window used in the operational DHW algorithm.

77 Alternate DHW algorithms have been applied to evaluate associations between heat stress and coral
78 bleaching, mostly at local or regional scales (Weeks et al. 2008; Guest et al. 2012; Kim et al. 2019;
79 McClanahan et al. 2020; Wyatt et al. 2020). Particularly for weak marine heatwaves associated with
80 coral bleaching, computing DHWs with a lower HotSpot threshold has proven useful for monitoring
81 bleaching impacts and severity (Guest et al. 2012; Kim et al. 2019; Wyatt et al. 2020). Evidence also
82 suggests that using a shorter accumulation window in the DHW algorithm can improve coral
83 bleaching predictions in some cases (DeCarlo 2020; McClanahan et al. 2020). An optimisation study
84 in which numerous DHW algorithms are tested against a global coral bleaching dataset could provide
85 the scientific basis necessary to revise the operational DHW metric. Recently, DeCarlo (2020) showed
86 that altering the HotSpot threshold and accumulation window can improve global coral bleaching
87 prediction skill, based on weather forecasting techniques that predict bleaching events (yes or no)
88 depending on whether DHWs exceed a certain threshold or not. DeCarlo used DHWs computed from
89 Optimum Interpolation SST (OI-SSTv2) and coral bleaching records from a summative dataset of 100
90 well-studied coral reefs (Hughes et al. 2018). However, there is a mismatch in spatial scale between
91 these two datasets; the SST data was extracted from 0.25-degree grid cells, while the area extent of
92 each reef in the bleaching dataset ranged from 2 km² (Southwest Rocks, Australia, and St. Lucia,

93 South Africa) to over 9000 km² (Northern Great Barrier Reef, Australia). Accordingly, there are
94 potential mismatches between DHW values and bleaching data in their study. As such, there is a
95 pressing need to apply a more comprehensive DHW optimisation study to a global dataset of direct
96 bleaching observations and DHWs derived from a higher resolution SST dataset.

97 To construct a global coral bleaching model based on environmental covariates, predictions should
98 account for spatial and temporal dependencies. For example, corals in certain geographic regions are
99 likely to respond to heat stress with higher levels of coral bleaching (e.g., areas influenced by the El
100 Niño Southern Oscillation) (Howells et al. 2016; Romero-Torres et al. 2020) and are likely to change
101 through time due to coral adaptation and assemblage turnover (Dziedzic et al. 2019; Gouezo et al.
102 2019). From a statistical standpoint, spatiotemporal uncertainties in the bleaching–environment
103 relationship must be accounted for to ensure that bleaching predictions are not just artefacts of spatial
104 or temporal patterns in unmeasured variables. A number of studies modelling coral bleaching globally
105 as a function of environmental covariates have assumed that the uncertainty of this relationship is
106 spatiotemporally constant (Safaie et al. 2018; DeCarlo 2020). This assumption is unlikely to be true
107 for coral bleaching responses, given the potential for coral adaptation (Bay et al. 2017; Matz et al.
108 2018) and the extent to which post-disturbance turnover can alter the composition of the coral
109 assemblage (Gouezo et al. 2019) and therefore its tendency to experience subsequent coral bleaching.
110 To address the spatial issues (but not temporal), Sully et al. (2019) introduced a Bayesian mixed
111 modelling approach that explicitly resolved spatial variability in the uncertainty of bleaching–
112 environment relationships. This was achieved by treating ecoregion and site as hierarchical random
113 effects, but this comes at the cost of slow run-time, an issue further compounded by implementing
114 these models via Monte Carlo Markov Chains (MCMC) which run iteratively and slowly (Rue et al.
115 2009). Given these issues, such an approach would not be appropriate for a coral bleaching
116 optimisation study that aims to test hundreds of DHW algorithms whilst also accounting for spatial
117 and temporal dependencies, since such a study would require a prohibitively large amount of
118 computing resources.

119 This study seeks to offer a potential revision to the operational NOAA DHW metric with a view to
120 improving its ability to predict mass coral bleaching. This will require a suitable methodology that is
121 robust to spatiotemporal correlated uncertainties and runs with reasonable computational speed. Here,
122 we apply an alternative approach to modelling bleaching–environment relationships based on
123 Integrated Nested Laplace Approximation (INLA), which explicitly solves spatial and temporal
124 uncertainties with much greater computational speed than MCMC (Rue et al. 2009). We aim to
125 optimise two DHW algorithm parameters, the HotSpot threshold (from MMM – 4 to + 4°C) and the
126 accumulation window (from 2 to 52 weeks) to improve coral bleaching predictions globally whilst
127 still addressing the common issue of spatial and temporal dependencies. We achieved this by
128 combining recently developed Bayesian hierarchical modelling techniques using INLA with a
129 streamlined parallel-computing workflow on a high-performance computing cluster called “The
130 Rocket”. This allowed hundreds of spatiotemporal INLA models to be run in a short time frame (i.e.,
131 hours instead of weeks as would be the case using MCMC).

132 **Data & Methods**

133 *Coral Bleaching Data*

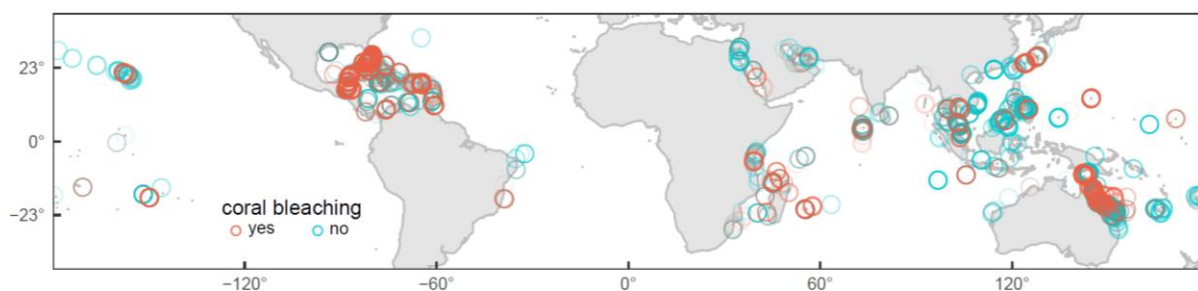
134 The optimisation study presented here was based on a global dataset of 37,871 bleaching survey
135 records from published and unpublished scientific sources spanning from 1969 to 2017 (Spady et al.
136 2021). Bleaching estimates were quantified by a wide range of surveying methods, including aerial
137 surveys, line-intercept transects, belt transects, quadrats, radius plots, rapid visual assessments (e.g.,

138 manta tows), ad hoc estimates, and interviews with stakeholders. Since data were collected by
139 hundreds of observers globally over several decades, data collection protocols for these different
140 general methods are not standardised.

141 The original dataset underwent four layers of filtering *a priori* to ensure its suitability for
142 analyses. 1) Data were first filtered for errors. This excluded observations that did not have a recorded
143 month or year, as well as observations in which the coordinates provided did not correspond with a
144 coral reef location (5,562 observations excluded). 2) Data were removed if the survey date fell outside
145 the period of peak thermal exposure for that year. As, for the purpose of this study, we are only
146 interested in coral bleaching that results from thermal stress (i.e., not bleaching due to cold-stress,
147 nutrient enrichment etc.), instances of bleaching that cannot be linked to the period of peak thermal
148 exposure may not accurately reflect the status of heat-induced bleaching for that year and location.
149 We defined the period of peak thermal exposure as the month prior to the month of MMM up to three
150 months after the month of MMM. For example, if the month of MMM was February for a certain
151 location, only observations from January-May were included. Further, we ensured that the observation
152 was not made before the date of maximum DHW in that year (19,292 observations excluded). 3) To
153 account for different sampling protocols in records of percentage bleaching, we computed bleaching
154 as a binary variable. Bleaching estimates were reported as means, ranges, or broad categories. First,
155 we summarised these as representative minimum and maximum percentages. Then, the absence of
156 ecologically significant bleaching was defined as having a maximum estimation of 10% bleaching or
157 less, while the presence of ecologically significant bleaching was defined as having a minimum
158 estimation of 20% or greater. Observations in which the maximum estimation exceeded 10% while
159 the minimum estimation remained below 20% were filtered out to reduce the chance of
160 misrepresenting bleaching and no-bleaching observations (Fig. S1) (1,452 observations excluded). 4)
161 Lastly, to account for spatiotemporal patchiness *a priori*, we only retained years which had greater
162 than 100 independent observations, had a qualitatively even global distribution, and were not
163 temporally isolated (i.e., the preceding years also needed to meet the previous two criteria). This
164 resulted in removal of all data before 2003. Despite having 345 bleaching records in 2002, all data
165 from this year were removed as over 80% of records were from the Great Barrier Reef region alone
166 (1,185 observations excluded). The resulting dataset included 10,380 unique observations between
167 2003 and 2017, with >171 observations per year and sufficient spatial representation for each year.

168 Accumulated heat stress is considered to be the mechanism causing mass coral bleaching (Heron et al.
169 2016; Skirving et al. 2019), and marine heatwaves typically occur across hundreds to thousands of
170 kilometres on spatial scales of weather-systems. The vast majority of bleaching observations in the
171 dataset are associated with mass bleaching events, but despite our filtration process, some bleaching
172 observations will inevitably result from small scale local heat stress and other non-heat related factors.
173 Since the models presented in this study are based solely on large scale accumulated heat stress, the
174 model predictions we present reflect the mechanism of mass coral bleaching which is referred to from
175 here on.

176



178 **Figure 1.** Distributions of coral bleaching survey records based on estimates of percentage coral
179 bleaching (< 10% = no, > 20% = yes), measured at 5724 sites from 84 countries between 2003 and
180 2017 (N = 10,380) after four layers of *a priori* filtering (i.e., removal of errors, matching surveys with
181 the period of peak thermal exposure in the year, accounting for inconsistent sampling protocols, and
182 accounting for spatiotemporal patchiness).

183 Temperature Data

184 Heat stress metrics were derived from a combination of CoralTemp v3.1 (Skirving et al. 2020), a gap-
185 free global 5km daily SST dataset from 1985 until present, and corresponding 5km MMM
186 climatology (Skirving et al. 2020). At each spatially referenced survey record, environmental data
187 were extracted from the 5km grid cell encompassing that coordinate. These data consisted of a single
188 MMM value and a time series of daily SST from the start of the pre-survey year until the end of the
189 survey year.

190 For the operational DHW metric used by NOAA (DHW_{op}), daily HotSpots were calculated as daily
191 positive SST anomalies relative to MMM (1). Time series of daily DHW_{op} were then computed using
192 the standard NOAA CRW method (2). HotSpots greater than 1°C were accumulated across a 12-week
193 moving window (84 days inclusive), where *i* is the date and *n* is the earliest date of the accumulation
194 window. Each daily HotSpot used in the summation is divided by seven a priori, such that

$$HotSpot_i = SST_i - MMM, \quad HotSpot_i \geq 0 \quad (1)$$

$$Operational\ DHW_i = \sum_{n=i-83}^i \left(\frac{HotSpot_n}{7} \right), \quad for\ HotSpot_n \geq 1 \quad (2)$$

195 As an example, consider a 12-week window ending on April 1st for a specific survey location. This
196 window includes only three daily SSTs that exceed the MMM, equivalent to HotSpots of 0.5, 1.4, and
197 2.8°C. The DHW_{op} value for April 1st is the summation of 1.4 and 2.8°C each divided by seven,
198 which is 0.6°C-weeks. The 0.5°C HotSpot value was not included in the summation as it was below
199 1°C (Skirving et al. 2020).

200 We computed a total of 234 test DHW metrics (DHW_{test}), each with unique combinations of HotSpot
201 thresholds (9 levels, from -4 to +4°C relative to MMM) and accumulation windows (26 levels, from
202 2 to 52 weeks). Unlike the operational metric, HotSpots for DHW_{test} were calculated relative to the
203 MMM after an adjustment for the specific threshold in question (3). In the operational metric only
204 HotSpots > 1°C are accumulated, however, in the test metrics all positive HotSpots are accumulated.
205 Therefore, values of DHW_{test} are numerically different than DHW_{op} but are conceptually the same (see
206 Figure 6). Time series of daily DHW_{test} were computed as the accumulation of HotSpots (4), where *i*
207 is the date, *n* is the earliest date of the accumulation window, and *j* is the length of the accumulation
208 window in days minus one, such that

$$HotSpot_i = SST_i - MMM + HotSpot\ Threshold, \quad HotSpot_i \geq 0 \quad (3)$$

$$Test\ DHW_i = \sum_{n=i-j}^i \left(\frac{HotSpot_n}{7} \right), \quad for\ HotSpot_n \geq 0 \quad (4)$$

209

210 Statistical Approach

211 The time unit used in the following models is the calendar year. As coral bleaching is more likely at
212 higher levels of heat stress (Heron et al. 2016), the maximum of daily DHW values was computed

213 from the year of each survey record. Thus, all further reference to DHW metrics relate to the annual
214 maximum summary statistic. Given that the southern hemisphere summer starts before the end of the
215 calendar year, there was a chance of misclassifying maximum DHW values. For instance, a maximum
216 DHW on the first or last day of a calendar year will be part of the same heatwave event, however they
217 will each be assigned to different calendar years. Previously, this has been addressed by adopting
218 different calendars for each hemisphere (Skirving et al. 2019), however, this was not necessary in the
219 current study since no such instances were present in the dataset. The relative performance of DHW
220 metrics for predicting mass coral bleaching were assessed systematically using the following
221 conceptual framework.

- 222 1) For each DHW metric, the association with coral bleaching was tested using a spatiotemporal
223 Generalised Linear Model (GLM) with a Bernoulli error structure using INLA.
- 224 2) Sensitivity-specificity analysis was performed on this GLM to optimise predictions, tally
225 model successes and failures, and provide metrics for model comparisons.
- 226 3) The first two steps were repeated for all DHW_{test} metrics and DHW_{op} , resulting in 235
227 separate GLMs and sensitivity-specificity analyses, each run in parallel on separate Intel
228 Xeon E5-2699 processors via the high-performance computing cluster “The Rocket”.
- 229 4) Model comparisons were used to determine the best-performing models and hence the
230 optimal HotSpot threshold and accumulation window for predicting coral bleaching globally
231 using DHWs.

232 Model formulation

233 We have adopted a spatiotemporal Bayesian modelling approach to predict mass coral bleaching
234 based on DHWs using the R-INLA package (<http://www.r-inla.org>) (Rue et al. 2009). Compared to
235 more commonly used frequentist approaches, Bayesian inference allows uncertainty to be more easily
236 interpreted. Moreover, using R-INLA over other Bayesian tools (e.g., Monte Carlo Markov Chains)
237 provides the opportunity to resolve spatiotemporal correlation explicitly and more rapidly (Rue et al.
238 2009).

239 Observations of mass coral bleaching are often spatiotemporally correlated due to large-scale climatic
240 drivers. While basic linear regressions applied to such data ignore these dependencies and lead to
241 pseudoreplication (Hulbert 1984), R-INLA circumvents these issues. In each time point, spatial
242 dependencies are dealt with by implementing the Matérn correlation across a Gaussian Markov
243 random field (GMRF), essentially a map of spatially correlated uncertainty. This is achieved using
244 stochastic partial differential equations (SPDE) solved on a Delaunay triangulation mesh of the study
245 area. The parameters (Ω) that determine the Matérn correlation are the range (r – range at which
246 spatial correlation diminishes) and error (σ). Weakly informative prior estimates of these parameters
247 (r_0 and σ_0) are recommended when implementing the Matérn correlation (Fuglstad et al. 2019).
248 Temporal dependencies among these GMRFs are dealt with by imposing a first order autoregressive
249 process (AR1), defined by the AR1 parameter (ρ) (9). This allows for correlation in model residuals
250 through time avoiding pseudoreplication.

251 To test the effect of DHW metrics on coral bleaching, a triangular mesh (Fig. 2) was defined with a
252 maximum triangle edge length of 600 km and a low-resolution convex hull (convex = -0.03) around
253 the study sites to avoid boundary effects (1,790 nodes). This mesh was repeated for each year in the
254 time series (26,400 nodes). The probability of coral bleaching for a given observation ($CB_{t,i}$) in a
255 given year (t) and location (i) was assumed to follow a Bernoulli distribution ($\pi_{t,i}$) using the logit-link
256 function for binary data. Bleaching was modelled as a function of the DHW metric in question (fixed
257 effect: $DHW_{t,i}$) whilst accounting for additional underlying spatiotemporal correlation among
258 bleaching observations (random effect: $v_{t,i}$),

259 $CB_{t,i} \sim \text{Bernoulli}(\pi_{t,i}),$ (5)

260 $\text{Expected}(CB_{t,i}) = \pi_{t,i},$ (6)

261 $\text{Variance}(CB_{t,i}) = \pi_{t,i} \times (1 - \pi_{t,i}),$ (7)

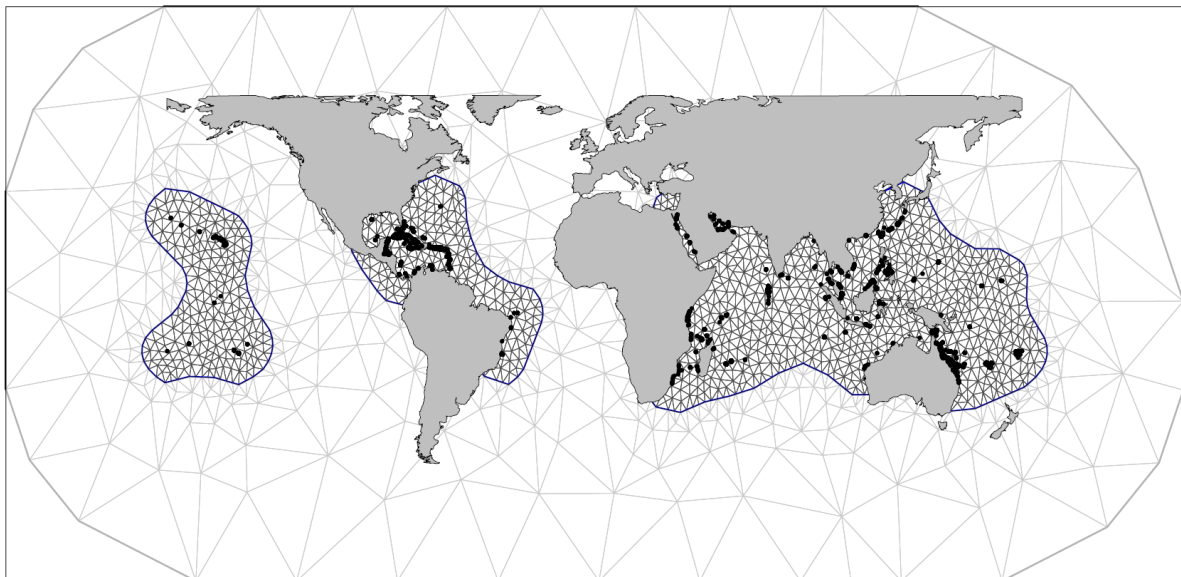
262 $\text{logit}(\pi_{t,i}) = \beta_0 + \beta_1 \times \text{DHW}_{t,i} + v_{t,i} + \varepsilon_{t,i},$ (8)

263 $v_{t,i} = \rho \times v_{t-1,i} + u_{t,i},$ (9)

264 $u_{t,i} \sim \text{GMRF}(0, \Omega),$ (10)

265 $\varepsilon_{t,i} \sim N(0, \sigma^2),$ (11)

266 where β_0 is the intercept, β_i is the DHW parameter estimate, ρ is the AR1 parameter, $u_{t,i}$ represents the
267 smoothed spatial effect from the GMRF mesh, elements of Ω (r and σ) are estimated from the Matérn
268 correlation, and $\varepsilon_{t,i}$ contains the independently distributed residuals. Following the recommendations
269 from Fuglstad et al. (2019), we specified weakly informative priors for r_0 (2000 km) and σ_0 (1.15)
270 based on the residual variogram and error from an intercept-only null Bernoulli GLM (Fig. S2). We
271 also tested different priors; however, they had a negligible effect on the estimates of any model
272 parameters. To avoid imposing artificial temporal dependencies, we used a non-informative default
273 prior for ρ .



274

275 **Figure 2.** Constrained refined Delaunay triangulation mesh of 1790 nodes used for spatial correlation
276 in one timestep. The spatiotemporal correlation over 15 years is computed over 15 such meshes
277 totalling 26,400 nodes. Continents and bleaching survey coordinates (black points) overlay the higher
278 resolution study area (black mesh) and lower resolution convex hull (grey mesh).

279 Model Validation

280 Standard model validation steps were conducted for the best performing GLM and included plotting
281 bleaching observations against fitted values, assessing model residuals for spatiotemporal correlation
282 using maps and variograms, and producing a time series of maps showing spatiotemporally correlated
283 uncertainty (Zuur and Ieno 2017). The dataset presented here was considerably patchy in both space
284 and time despite prior filtering (e.g., no South Pacific observations in 2003, 2012, or 2013). Patchy
285 data is a pertinent issue in statistics (Little and Rubin 2002) and can have a considerable effect on

286 estimated model parameters (Bihmann and Ersbøll 2015), and model selection criteria (e.g.,
287 Deviance Information Criterion – DIC) (Nakagawa and Freckleton 2008). Thus, to address patchiness
288 beyond basic filtering, we performed a simulation test (Fig. S3 & Fig. S4). In summary, patchiness
289 did not have an important effect on estimated model parameters (Fig. S5), validating the broader
290 model comparison methods and results of the main study. Full details are described in the
291 Supplementary Materials.

292 Sensitivity-Specificity Analysis

293 To optimise binary predictions from each Bernoulli GLM, sensitivity-specificity analyses were
294 performed using receiver operating characteristic (ROC) curves in R (Robin et al. 2011) without
295 considering spatiotemporal dependencies. This method is commonly applied in bioinformatics and
296 medical decision making to determine the performance of binary classifications. Here, sensitivity is
297 defined as the proportion of correctly classified bleaching observations (true positives), and specificity
298 as the proportion of correctly classified no-bleaching observations (true negatives). As a probability
299 cut-off is moved over all possible values, the ROC plot shows the corresponding sensitivity and
300 specificity at each level. The Area Under the Curve (AUC) from each ROC plot reflects the
301 performance of that GLM relative to the perfect predictor (AUC = 1) and can be used for multi-model
302 comparisons based on 95% confidence intervals computed using stratified bootstrap resampling
303 (Robin et al. 2011). The hit rate, defined as the proportion of observed bleaching events that were
304 correctly predicted, was also computed at the optimal cut-off level for each model.

305 Model Comparisons

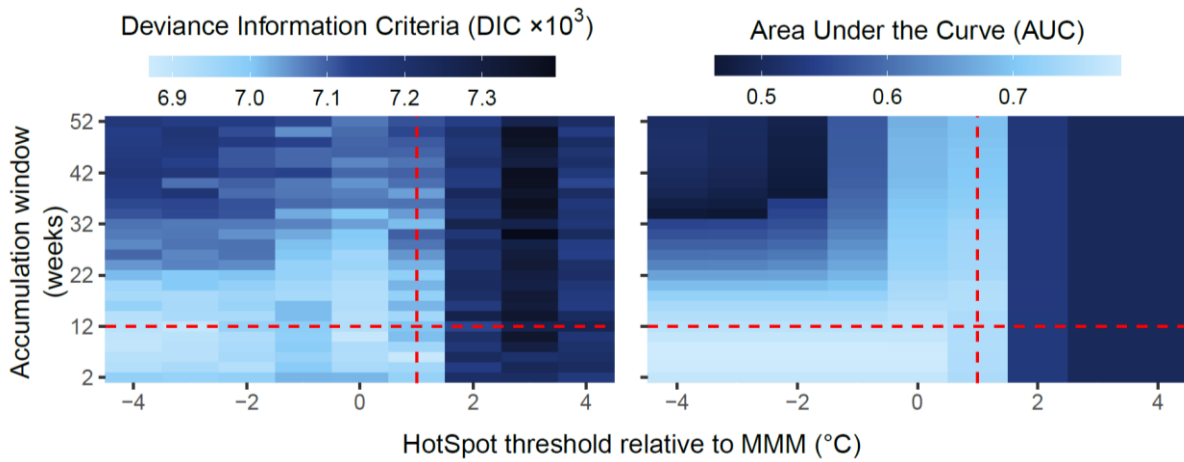
306 Model comparisons were based on the Bayesian DIC and two key metrics from the sensitivity-
307 specificity analysis: AUC and hit rate. DIC is a measure of overall model parsimony (Zuur and Ieno
308 2017), but is based on both the DHW fixed effect and the spatiotemporal random effect. Therefore,
309 AUC and bootstrapped confidence intervals were used as the preferred model comparison metric, as
310 this evaluates the overall performance of a binary classifier relative to a perfect predicting model
311 (Robin et al. 2011), based on the fixed effect only. Hit rate is an additional metric that allows easy
312 interpretation of model success.

313 **Results**

314 Model Comparisons

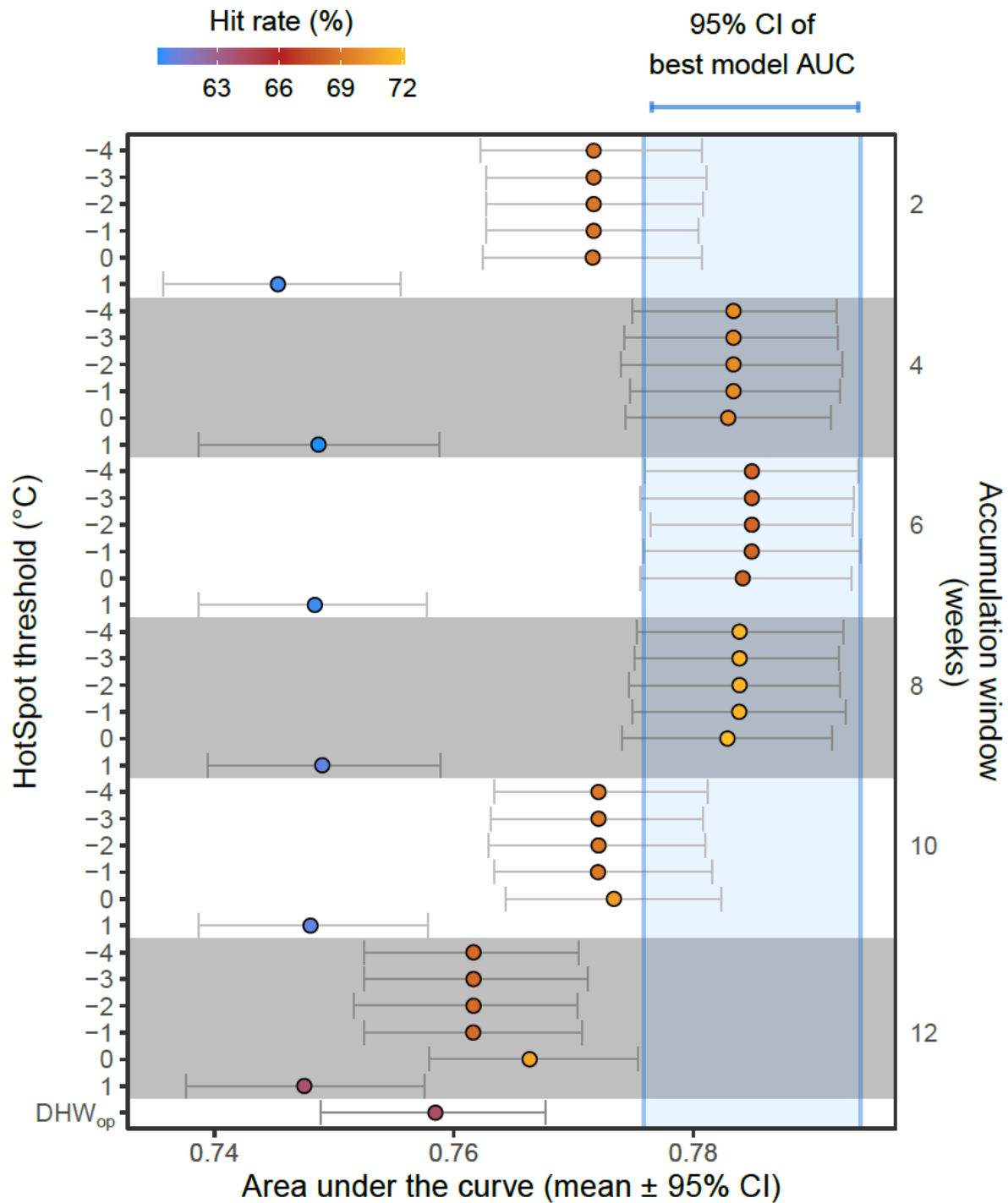
315 For predicting coral bleaching based on DHW_{test} , we identify (1) a group of worst performing models,
316 (2) a group of better performing models, and (3) a suite of best performing models. (1) Poor GLM
317 performance was associated with DHW_{test} metrics computed on HotSpot thresholds $\geq MMM + 2^{\circ}C$ or
318 accumulation windows ≥ 22 weeks. This was evident by low AUC values < 0.7 and high DIC values
319 > 7000 (Fig. 3, right and upper regions). (2) The remaining GLMs (HotSpot threshold $\leq MMM + 1^{\circ}C$,
320 accumulation window ≤ 20 weeks) were associated with better coral bleaching predictions (AUC) and
321 model parsimony (DIC) (Fig. 3, lower and lower left regions). (3) Finer determination of the best
322 models of this subset was made possible by incorporating sensitivity-specificity uncertainty into
323 model comparisons (Fig. 4, 95% bootstrapped confidence intervals). A performance-optima
324 relationship was apparent between AUC and the HotSpot threshold and accumulation window,
325 whereby peak GLM performance was reached when DHW accumulation windows were 4 – 8 weeks
326 (Fig. 4). When DHW accumulation windows were outside this range (2 weeks or ≥ 10 weeks),
327 corresponding AUC was significantly lower than the AUC of the best performing GLMs (Fig. 4, blue
328 shaded region). Notably, of all the GLMs that used the same accumulation window (grey and white
329 band groupings, Fig. 4), those models applying lower HotSpot thresholds performed better in terms of
330 AUC and DIC. The 8-week accumulation window resulted in the best overall fit of AUC and DIC

331 combined (max DIC = 6812). In summary, the suite of best-performing models (in terms of bleaching
332 prediction) applied DHW_{test} metrics based on HotSpot thresholds \leq MMM and accumulation windows
333 of 4 – 8 weeks.



334

335 **Figure 3.** Model comparison heatmaps showing the Deviance Information Criterion (DIC) and Area
336 Under the Curve (AUC) for 234 Generalised Linear Models (GLMs) that each predict coral bleaching
337 based on a different DHW_{test} metric. Raster cells represent individual GLMs plotted by HotSpot
338 threshold and accumulation window. The threshold and window used for DHW_{op} are shown by red
339 dashed lines (MMM + 1°C, and 12-weeks). Results for the DHW_{op} GLM are not shown on the heat
340 maps (DIC = 6967, AUC = 0.758).

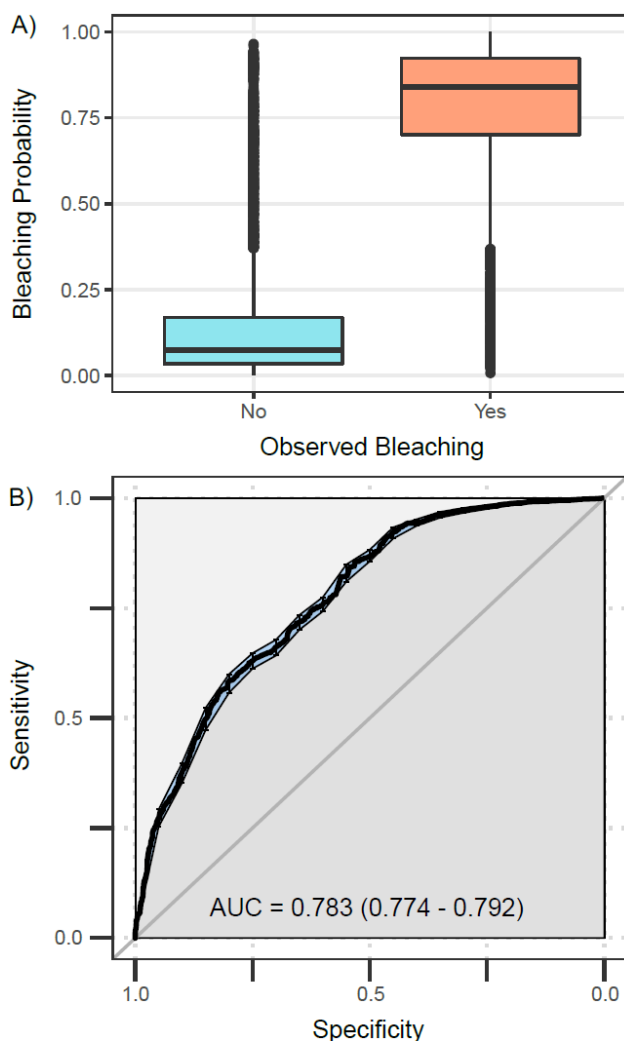


341

342 **Figure 4.** Model comparisons accounting for uncertainty in Area Under the Curve (AUC) showing
 343 the mean and 95% bootstrapped confidence intervals (CI). Each point represents a Generalised Linear
 344 Model GLM that predicts coral bleaching based on a different DHW_{test} metric, ordered by HotSpot
 345 threshold and accumulation window (both increasing downwards). The hit rate (proportion of
 346 observed bleaching events correctly predicted) is shown for each GLM (point colour) and the AUC of
 347 the best GLM is shown as a blue shaded region. Note the DHW_{op} algorithm is slightly different than
 348 the DHW_{test} algorithm (Equation 1-4).

349 *Best Model – Validation*

350 The GLM based on the DHW_{test} metric with HotSpot threshold of $MMM + 0^{\circ}C$ and accumulation
351 window of 8 weeks ($DHW_{test-0C-8wk}$), was a representative of the suite of best-performing models. The
352 probability of bleaching output from this model (based on $DHW_{test-0C-8wk}$ and unmeasured
353 spatiotemporally correlated factors) closely matched the observational bleaching record (Fig. 5A).
354 Both the fixed effect ($DHW_{test-0C-8wk}$) and the random effect (spatiotemporal uncertainty) provided
355 important contributions to predictions of coral bleaching (Fig. S7). The sensitivity-specificity analysis
356 reflected the high performance for this model, with an AUC value of 0.783 (Fig. 5B). The range
357 parameter (r) of GMRFs showed that drivers of bleaching other than $DHW_{test-0C-8wk}$ were spatially
358 correlated up to 697 km (Fig. S6), consistent with the spatial scale of climatic and weather systems.
359 The AR1 parameter (ρ) of 0.62 indicated moderate temporal correlation of uncertainty in predicted
360 coral bleaching (i.e., drivers other than $DHW_{test-0C-8wk}$), meaning that the uncertainty in bleaching
361 predictions in one year is affected by that of the previous year by a factor of 0.62 (Fig. S6). This can
362 be seen visually on maps of temporally correlated GMRFs (Fig. S7).



363

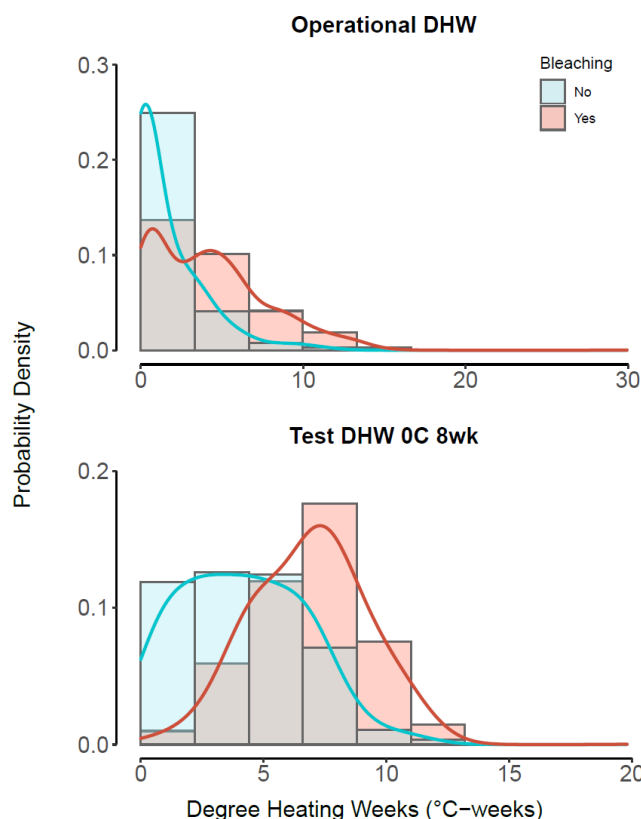
364 **Figure 5.** Exploration of best-performing GLM which predicts coral bleaching based on $DHW_{test-0C-}$
365 $8wk$ (HotSpot threshold = MMM , accumulation window = 8 weeks) and spatiotemporal uncertainty.
366 (A) Fitted values or bleaching probabilities are shown relative to bleaching observations from the
367 global dataset, showing a clear separation between bleaching and non-bleaching categories. (B)
368 Sensitivity-specificity analysis is shown for the same GLM without spatiotemporal uncertainty.
369 Sensitivity is defined as the proportion of correctly classified bleaching observations (true positives),
370 and specificity as the proportion of correctly classified no-bleaching observations (true negatives).

371 Area Under the Curve (AUC) and bootstrapped 95% confidence intervals (shown in brackets) reflect
372 the distance to a perfect predicting model (AUC = 1).

373 Best Model – Understanding Heat Stress

374 Even though lowering the HotSpot threshold and reducing the accumulation window improved
375 predictions of mass coral bleaching (Fig. 3, Fig. 4), the DHW_{op} metric still categorised bleaching
376 observations well. DHW_{op} values were greater for bleaching records than for non-bleaching records
377 (Fig. 6). Of the 517 highest heat stress records ($> 95^{th}$ percentile: $> 9.0^{\circ}C$ -weeks), 78% were
378 associated with coral bleaching observations, highlighting the importance of heat stress as a proximate
379 cause of coral bleaching. Such levels of heat stress relate to NOAA CRW Bleaching Alert Level 2.
380 However, in comparison to DHW_{op} , the test metric $DHW_{test-0C-8wk}$ showed a higher distribution of heat
381 stress values overall, but lower extremes values (Fig. 6). This is due to a lower HotSpot threshold and
382 shorter accumulation window, respectively. This was characterised by fewer DHW values of zero (1
383 vs. 27%), a higher mean (5.2 vs. $2.5^{\circ}C$ -weeks), a higher 95^{th} percentile (9.9 vs. $9.0^{\circ}C$ -weeks), but a
384 lower 99^{th} percentile (11.3 vs. $12.5^{\circ}C$ -weeks). The number of bleaching observations associated with
385 a heat stress of zero was 6 for $DHW_{test-0C-8wk}$ and 122 for DHW_{op} . Given that $DHW_{test-0C-8wk}$ had a
386 lower HotSpot threshold, fewer bleaching observations are associated with heat stress values of zero.
387 In other words, reducing the HotSpot threshold increased our ability to predict coral bleaching
388 associated with weak marine heatwaves.

389



390

391 **Figure 6.** DHW distributions for bleaching records (red) and non-bleaching records (blue), shown as
392 histograms and probability density curves. For comparison of different DHW metrics, the operational
393 metric used by NOAA (DHW_{op}) is shown alongside one of the best-performing metrics ($DHW_{test-0C-}$
394 $8wk$), calculated using a lower HotSpot threshold ($MMM + 0^{\circ}C$) and a smaller accumulation window
395 (8 weeks).

396 Discussion

397 Heat stress can have considerable impacts on marine organisms and entire marine ecosystems (Eakin
398 et al. 2019; Smale et al. 2019). The DHW metric is a measure of accumulated heat stress widely used
399 to predict mass coral bleaching caused by anomalous temperatures above typical summertime
400 conditions (Heron et al. 2016; Safaie et al. 2018; Skirving et al. 2019; Sully et al. 2019). The remote-
401 sensed SST products underpinning the operational NOAA DHW metric have improved stepwise over
402 the last two decades (Wellington et al. 2001; Liu et al. 2003; Liu et al. 2013; Skirving et al. 2020),
403 however, there has not yet been a corresponding revision of the HotSpot threshold and accumulation
404 window used in this algorithm. Here, we developed 234 different DHW algorithm variants each with
405 a different HotSpot threshold and accumulation window. We assess the performance of these DHW_{test}
406 metrics for predicting mass coral bleaching globally. Compared to DHW_{op}, it was possible to improve
407 the coral bleaching hit-rate by up to 7.9% by using different HotSpot thresholds and accumulation
408 windows, equating to an additional 310 correctly predicted bleached reefs out of a total of 3895 (also
409 linked to an increased false negative rate of 3%). Simply reducing the HotSpot threshold to MMM (or
410 < MMM) rather than MMM + 1°C, resulted in up to 6.8% increases in hit rate, whilst using an
411 accumulation window of 8 weeks instead of 12 weeks maximised this hit rate. Such improvements
412 were also reflected in model comparison metrics from sensitivity-specificity analyses (increased AUC
413 of 0.02) and Bayesian inference (decreased DIC of 36). Models using the 4 – 8 week accumulation
414 window generally performed best, reflecting the typical duration of the vast majority of coral
415 bleaching heat stress events to date (Oliver et al. 2018). Under climate change, however, average sea
416 temperatures and the duration of marine heatwaves are predicted to continue increasing (Hoegh-
417 Guldberg et al. 2018; Oliver et al. 2018), meaning in the future, longer DHW accumulation windows
418 may better capture the levels of heat stress relevant to coral bleaching. Given that baselines are
419 shifting throughout biotic and abiotic marine systems and that rates of adaptation to future
420 environmental conditions are yet unknown, the concepts addressed in this study likely need to be
421 revisited in the future at semi-regular intervals to ensure that the DHW product remains as accurate as
422 possible.

423 Complexities of coral bleaching

424 Coral bleaching is a stress response whereby photosynthetic algal symbionts are lost from the coral
425 host tissues, resulting in the white coral skeleton becoming progressively more visible (Brown 1997;
426 Douglas 2003). Given the complexity of this host-symbiont relationship, survey metrics such as ‘coral
427 bleaching extent’ provide limited information from which to infer biological causes. Coral bleaching
428 is affected by numerous biological factors including symbiont community composition and their
429 environmental responses (e.g., more or less heat-tolerant algal taxa) (LaJeunesse et al. 2018), host
430 heterotrophy (e.g., reliance on the symbiont) (Conti-Jerpe et al. 2020), the capacity for acclimation
431 and adaptation both genetic and epigenetic (intra- and inter-generational) (Kirk et al. 2018; Liew et al.
432 2020), and coral taxonomy (e.g., different life history strategies) (Marshall and Baird 2000; Guest et
433 al. 2012). In addition, other environmental factors can influence bleaching responses in corals, such as
434 high solar insolation, cloudiness, winds, tidal extremes, thermal variability, cold-water stress and
435 nutrient enrichment (Mumby et al. 2001; Hoegh-Guldberg et al. 2005; Anthony et al. 2007; Anthony
436 and Kerswell 2007; Wiedenmann et al. 2013; González-Espinosa and Donner 2020). Given this suite
437 of biotic and abiotic factors, a perfect-predicting coral bleaching algorithm would need to combine
438 heat-stress metrics with other environmental and biological parameters that in many cases are often
439 not available. NOAA CRW are investigating the potential improvements to DHW via the inclusion of
440 solar insolation with the development of their Light Stress Damage (LSD) satellite-based product
441 (Skirving et al. 2018).

442 Here we have refined the ability of a common heat stress metric to predict mass coral bleaching.
443 Ideally, such an optimisation study would be based on coral bleaching data that relate to only heat

444 stress related mechanisms. By filtering the dataset as described, we did our best to achieve this,
445 however, bleaching observations in the dataset may inevitably have been caused by other biotic or
446 abiotic factors, contributing to the noise in our results. Bleaching observations from surveys may also
447 be subject to other inaccuracies such as the assumption that sampling only part of a reef is
448 representative of the entire reef. Despite these points, the model comparisons performed in this study
449 remain valid as model biases were applied to all models equally. Given these facts, the AUC and hit
450 rate from sensitivity-specificity analyses are unlikely to reflect the absolute accuracy of DHW
451 metrics, but rather allow comparisons of relative accuracy to determine optimal HotSpot thresholds
452 and accumulation windows. The optimisation study presented here was performed on a global coral
453 bleaching dataset. For scientists and practitioners aiming to assess global patterns in coral bleaching,
454 we have shown that bleaching predictions can be improved by computing DHW metrics using an
455 optimal HotSpot threshold of the MMM + 0°C and accumulation window of 8 weeks. These
456 recommended DHW algorithm refinements are only applicable to global analyses and predictions of
457 mass coral bleaching caused by heat stress. Moreover, it is important to note that the quasi-
458 opportunistic nature of coral bleaching surveys (i.e., monitoring coral bleaching when DHW values
459 are high indicating high bleaching risk) can lead to a confirmation bias in studies of coral bleaching
460 and heat stress. Monitoring programmes should address this limitation, by aiming to survey bleaching
461 more regularly, even when there is no accumulated temperature stress (i.e., DHW = 0).

462 Global and regional scales

463 A regionally sensitive DHW algorithm would likely improve predictions of mass coral bleaching. For
464 instance, many scientific studies have used variants of the DHW algorithm to better predict coral
465 bleaching in their study site (Guest et al. 2012; Kim et al. 2019; Wyatt et al. 2019). This will likely
466 continue, since oceanographic and climatic systems, coral assemblages, and the distribution of algal
467 symbiont taxa vary geographically and at regional scales (Veron 1995; Clarke 2014; LaJeunesse et al.
468 2018). For instance, the thermal regime of the tropical Eastern Pacific is distinct from many other
469 tropical regions, characterised by high variability due to the El Niño Southern Oscillation, with more
470 intense warm water conditions typical of La Niña years compared to El Niño years (Clarke 2014).
471 Long-term trends in coral coverage from this region, which have remained very stable over the past 3
472 decades, are atypical compared to most tropical reefs which have suffered persistent declines (Hughes
473 et al. 2017; Romero-Torres et al. 2020). Such distinct trends in the tropical Eastern Pacific could be
474 caused by adaption of corals there to highly variable thermal regimes (Romero-Torres et al. 2020).
475 This is just one example of a region that could benefit from a specific regional DHW optimisation.
476 Notably, the methods applied in this study would be easily adapted to develop such regional DHW
477 products.

478 Future outlook

479 Optimising heat stress metrics for specific purposes could also be useful for other marine systems.
480 Marine heatwaves have contributed to marked ecological disturbances beyond mass coral bleaching
481 and mortality events (Ummenhofer and Meehl 2017; Frölicher and Laufkötter 2018; Smale et al.
482 2019), yet specific metrics to predict these other disturbances are not often implemented. The
483 northeast Pacific warming event of 2013 – 2015, termed “the blob”, was the subject of unusually high
484 SST anomalies and repeated marine heatwaves (Di Lorenzo and Mantua 2016). The blob was
485 associated with considerable ecological impacts, including the mass stranding of marine mammals
486 such as sea lion and whales (Cavole et al. 2016), die-offs and reproductive failure of seabird
487 populations (Cavole et al. 2016; Jones et al. 2018; Piatt et al. 2020), and reduced survival and growth
488 of foraging fish (von Biela et al. 2019). In all these cases, evidence suggested that declines in higher
489 trophic levels were associated not to direct effects of heat stress, but to the cascading effects of heat-
490 mediated declines at lower trophic levels. Reduced abundance and altered composition of zooplankton
491 communities including krill are highly susceptible to heat stress (Jiménez-Quiroz et al. 2019; Evans et

492 al. 2020; Işkın et al. 2020), which can result in reduced food availability for higher trophic level
493 animals (e.g., Cassin's auklet and Californian sea lion), their emaciation and mortality (Cavole et al.
494 2016). The urgency to understand the full extent of ecological impacts associated with marine
495 heatwaves could in part be addressed by creating new heat stress indicators that are optimised for
496 specific disturbances using similar methods to those applied here. While this would not allow for
497 rapid response actions to such events, it would guide marine protected area design (i.e., focus on
498 conserving thermal refugia) and inform future projections of marine systems and related policy
499 recommendations.

500 Conclusion

501 The Anthropocene is characterised by shifting baselines of biological communities, loss of
502 biodiversity, and increasingly severe and frequent climatic disturbances. Thus, there is growing need
503 to understand and be able to predict climatic and anthropogenic disturbances on habitats, particularly
504 those that provide key ecosystem services to socioecological systems. Here, we have fine-tuned a
505 commonly used heat stress algorithm to a specific purpose (i.e., predicting mass coral bleaching), and
506 have shown that simple changes (compared to the operational algorithm) can result in a considerable
507 improvement in prediction success. The philosophy behind this optimisation study was to remove
508 prior expectations, run the models, and allow the data to reveal the optimal HotSpot threshold and
509 accumulation window for predicting mass coral bleaching globally. In this case, coral bleaching
510 observations were correctly predicted up to 7.9% more often just by reducing the HotSpot threshold
511 and accumulation window of the DHW_{test} metric. Broadly, improving bleaching prediction success of
512 the operational DHW metric can support stakeholders and end-users such as coral reef managers,
513 inform the design of MPA networks (e.g., including thermal refugia), and provide more accurate
514 information which can lead to better conservation and restoration decision-making (e.g., shifting
515 valuable coral nurseries during heatwaves, assisting with decisions on when to relocate aquarium-
516 grown corals to the reef, etc.). Fine-tuning DHWs also has potential for other specific systems, such
517 as predicting planktonic shifts and associated impacts to higher trophic levels. Increasingly under
518 climate change, marine heatwaves are shaping species populations, biological food webs and even
519 ecosystem structure and function (Hughes et al. 2017; Eakin et al. 2019; Smale et al. 2019). Thus,
520 optimising our predictions of heat stress and the associated ecological impacts will be key to
521 understanding the future of marine ecosystems.

522 Acknowledgements

523 This research was funded by the Natural Environment Research Council's ONE Planet Doctoral
524 Training Partnership (NE/S007512/1) to L.L., the European Research Council Horizon 2020 project
525 CORALASSIST (Project number 725848) to J.R.G. and A.J.E. Coral Reef Watch and ReefSense staff
526 (B.L.S. and W.J.S.) were supported by NOAA grant NA19NES4320002 (Cooperative Institute for
527 Satellite Earth System Studies) at the University of Maryland/ESSIC, and the U.S. Department of
528 Defense's Strategic Environmental Research and Development Program. The authors would also like
529 to thank Dr. Adriana Humanes and Prof. Stephen Rushton for their intellectual contributions to the
530 study and methodology, and the innumerable divers, volunteers and citizen scientists who helped with
531 coral bleaching data collection. The scientific results and conclusions, as well as any views or
532 opinions expressed herein, are those of the author(s) and do not necessarily reflect the views of
533 NOAA or the Department of Commerce.

534 Author Contributions

535 L.L., J.C.B., A.J.E., J.R.G., and W.J.S. conceived and designed the study; the National Oceanic and
536 Atmospheric Administration Coral Reef Watch program provided the coral bleaching data and sea
537 surface temperature data; B.L.S., L.L., and W.J.S. accessed and filtered the datasets; L.L. developed
538 the models, prepared the figures, and wrote the code; L.L., and B.L.S. wrote the first draft of the

539 paper; and J.C.B., H.K.E., A.J.E., J.R.G., P.J.M., and W.J.S. contributed significantly to the
540 interpretation and editing of the manuscript.

541 **References**

- 542 Anthony KRN, Connolly SR, Hoegh-Guldberg O (2007) Bleaching, energetics, and coral mortality
543 risk: Effects of temperature, light, and sediment regime. *Limnol Oceanogr* 52:716–726 .
544 <https://doi.org/10.4319/lo.2007.52.2.0716>
- 545 Anthony KRN, Kerswell AP (2007) Coral mortality following extreme low tides and high solar
546 radiation. *Mar Biol* 151:1623–1631 . <https://doi.org/10.1007/s00227-006-0573-0>
- 547 Bay RA, Rose NH, Logan CA, Palumbi SR (2017) Genomic models predict successful coral
548 adaptation if future ocean warming rates are reduced. *Sci Adv* 3:1–10 .
549 <https://doi.org/10.1126/sciadv.1701413>
- 550 Bihmann K, Ersbøll AK (2015) Estimating range of influence in case of missing spatial data: A
551 simulation study on binary data. *Int J Health Geogr* 14: . [https://doi.org/10.1186/1476-072X-14-](https://doi.org/10.1186/1476-072X-14-1)
552 1
- 553 Brown BE (1997) Coral bleaching: Causes and consequences. *Coral Reefs* 16: .
554 <https://doi.org/10.1007/s003380050249>
- 555 Cavole LM, Demko AM, Diner RE, Giddings A, Koester I, Pagniello CMLS, Paulsen ML, Ramirez-
556 Valdez A, Schwenck SM, Yen NK, Zill ME, Franks PJS (2016) Biological impacts of the 2013–
557 2015 warm-water anomaly in the northeast Pacific: Winners, Losers, and the Future.
558 *Oceanography* 29:273–285 . <https://doi.org/10.5670/oceanog.2016.32>
- 559 Clarke AJ (2014) El Niño Physics and El Niño Predictability. *Ann Rev Mar Sci* 6:79–99 .
560 <https://doi.org/10.1146/annurev-marine-010213-135026>
- 561 Conti-Jerpe IE, Thompson PD, Wong CWM, Oliveira NL, Duprey NN, Moynihan MA, Baker DM
562 (2020) Trophic strategy and bleaching resistance in reef-building corals. *Sci Adv* 6: .
563 <https://doi.org/10.1126/sciadv.aaz5443>
- 564 Costanza R, de Groot R, Sutton P, van der Ploeg S, Anderson SJ, Kubiszewski I, Farber S, Turner RK
565 (2014) Changes in the global value of ecosystem services. *Glob Environ Chang* 26:152–158 .
566 <https://doi.org/https://doi.org/10.1016/j.gloenvcha.2014.04.002>
- 567 DeCarlo TM (2020) Treating coral bleaching as weather: a framework to validate and optimize
568 prediction skill. *PeerJ* 8:e9449 . <https://doi.org/10.7717/peerj.9449>
- 569 Di Lorenzo E, Mantua N (2016) Multi-year persistence of the 2014/15 North Pacific marine
570 heatwave. *Nat Clim Chang* 6:1042–1047 . <https://doi.org/10.1038/nclimate3082>
- 571 Donner SD, Heron SF, Skirving WJ (2018) Future Scenarios: A Review of Modelling Efforts to
572 Predict the Future of Coral Reefs in an Era of Climate Change. In: Oppen MJH van, Lough JM
573 (eds) *Coral Bleaching, Ecological Studies* 233, Second Edi. Springer International Publishing
574 AG, part of Springer Nature 2018, pp 325–341
- 575 Douglas AE (2003) Coral bleaching - How and why? *Mar Pollut Bull* 46:385–392 .
576 [https://doi.org/10.1016/S0025-326X\(03\)00037-7](https://doi.org/10.1016/S0025-326X(03)00037-7)
- 577 Dziedzic KE, Elder H, Tavalire H, Meyer E (2019) Heritable variation in bleaching responses and its
578 functional genomic basis in reef-building corals (*Orbicella faveolata*). *Mol Ecol* 28:2238–2253 .
579 <https://doi.org/10.1111/mec.15081>
- 580 Eakin CM, Sweatman HPA, Brainard RE (2019) The 2014–2017 global-scale coral bleaching event:
581 insights and impacts. *Coral Reefs* 38:539–545 . <https://doi.org/10.1007/s00338-019-01844-2>
- 582 Edmunds PJ (2005) The effect of sub-lethal increases in temperature on the growth and population
583 trajectories of three scleractinian corals on the southern Great Barrier Reef. *Oecologia* 146:350–
584 364 . <https://doi.org/10.1007/s00442-005-0210-5>

- 585 Evans R, Lea MA, Hindell MA, Swadling KM (2020) Significant shifts in coastal zooplankton
586 populations through the 2015/16 Tasman Sea marine heatwave. *Estuar Coast Shelf Sci*
587 235:106538 . <https://doi.org/10.1016/j.ecss.2019.106538>
- 588 Ferrario F, Beck MW, Storlazzi CD, Micheli F, Shepard CC, Airoidi L (2014) The effectiveness of
589 coral reefs for coastal hazard risk reduction and adaptation. *Nat Commun* 5:1–9 .
590 <https://doi.org/10.1038/ncomms4794>
- 591 Frölicher TL, Laufkötter C (2018) Emerging risks from marine heat waves. *Nat Commun* 9:2015–
592 2018 . <https://doi.org/10.1038/s41467-018-03163-6>
- 593 Fuglstad GA, Simpson D, Lindgren F, Rue H (2019) Constructing Priors that Penalize the Complexity
594 of Gaussian Random Fields. *J Am Stat Assoc* 114:445–452 .
595 <https://doi.org/10.1080/01621459.2017.1415907>
- 596 Glynn PW, D’Croz L (1990) Experimental evidence for high temperature stress as the cause of El
597 Niño-coincident coral mortality. *Coral Reefs* 8:181–191 . <https://doi.org/10.1007/BF00265009>
- 598 González-Espinosa P, Donner S (2020) Cold-water coral bleaching prediction: role of temperature,
599 and potential integration of light exposure. *Mar Ecol Prog Ser* 642:133–146 .
600 <https://doi.org/10.3354/meps13336>
- 601 Gouezo M, Golbuu Y, Fabricius K, Olsudong D, Mereb G, Nestor V, Wolanski E, Harrison P,
602 Doropoulos C (2019) Drivers of recovery and reassembly of coral reef communities. *Proc R Soc*
603 *B Biol Sci* 286: . <https://doi.org/10.1098/rspb.2018.2908>
- 604 Guest JR, Baird AH, Maynard JA, Muttaqin E, Edwards AJ, Campbell SJ, Yewdall K, Affendi YA,
605 Chou LM (2012) Contrasting patterns of coral bleaching susceptibility in 2010 suggest an
606 adaptive response to thermal stress. *PLoS One* 7:1–8 .
607 <https://doi.org/10.1371/journal.pone.0033353>
- 608 Heron SF, Johnston L, Liu G, Geiger EF, Maynard JA, De La Cour JL, Johnson S, Okano R,
609 Benavente D, Burgess TFR, Iguel J, Perez DI, Skirving WJ, Strong AE, Tirak K, Eakin CM
610 (2016) Validation of Reef-Scale Thermal Stress Satellite Products for Coral Bleaching
611 Monitoring. *Remote Sens* 8:
- 612 Hoegh-Guldberg O, Fine M, Skirving W, Johnstone R, Dove S, Strong A (2005) Coral bleaching
613 following wintry weather. *Limnol Oceanogr* 50:265–271 .
614 <https://doi.org/10.4319/lo.2005.50.1.0265>
- 615 Hoegh-Guldberg O, Jacob D, Taylor M, Guillén Bolaños T, Bindi M, Brown S, Camilloni IA,
616 Diedhiou A, Djalante R, Ebi K, Engelbrecht F, Guiot J, Hijioka Y, Mehrotra S, Hope CW,
617 Payne AJ, Pörtner HO, Seneviratne SI, Thomas A, Warren R, Zhou G (2019) The human
618 imperative of stabilizing global climate change at 1.5°C. *Science* (80-) 365: .
619 <https://doi.org/10.1126/science.aaw6974>
- 620 Hoegh-Guldberg O, Kennedy E V., Beyer HL, McClennen C, Possingham HP (2018) Securing a
621 Long-term Future for Coral Reefs. *Trends Ecol Evol* 33:936–944 .
622 <https://doi.org/10.1016/j.tree.2018.09.006>
- 623 Holbrook NJ, Scannell HA, Sen Gupta A, Benthuisen JA, Feng M, Oliver ECJ, Alexander L V.,
624 Burrows MT, Donat MG, Hobday AJ, Moore PJ, Perkins-Kirkpatrick SE, Smale DA, Straub SC,
625 Wernberg T (2019) A global assessment of marine heatwaves and their drivers. *Nat Commun*
626 10:1–13 . <https://doi.org/10.1038/s41467-019-10206-z>
- 627 Howells EJ, Abrego D, Meyer E, Kirk NL, Burt JA (2016) Host adaptation and unexpected symbiont
628 partners enable reef-building corals to tolerate extreme temperatures. *Glob Chang Biol* 22:2702–
629 2714 . <https://doi.org/10.1111/gcb.13250>
- 630 Hughes TP, Anderson KD, Connolly SR, Heron SF, Kerry JT, Lough JM, Baird AH, Baum JK,
631 Berumen ML, Bridge TC, Claar DC, Eakin CM, Gilmour JP, Graham NAJ, Harrison H, Hobbs
632 JPA, Hoey AS, Hoogenboom M, Lowe RJ, McCulloch MT, Pandolfi JM, Pratchett M, Schoepf

- 633 V, Torda G, Wilson SK (2018) Spatial and temporal patterns of mass bleaching of corals in the
634 Anthropocene. *Science* (80-) 359:80–83 . <https://doi.org/10.1126/science.aan8048>
- 635 Hughes TP, Kerry JT, Álvarez-Noriega M, Álvarez-Romero JG, Anderson KD, Baird AH, Babcock
636 RC, Beger M, Bellwood DR, Berkelmans R, Bridge TC, Butler IR, Byrne M, Cantin NE,
637 Comeau S, Connolly SR, Cumming GS, Dalton SJ, Diaz-Pulido G, Eakin CM, Figueira WF,
638 Gilmour JP, Harrison HB, Heron SF, Hoey AS, Hobbs JPA, Hoogenboom MO, Kennedy E V.,
639 Kuo CY, Lough JM, Lowe RJ, Liu G, McCulloch MT, Malcolm HA, McWilliam MJ, Pandolfi
640 JM, Pears RJ, Pratchett MS, Schoepf V, Simpson T, Skirving WJ, Sommer B, Torda G,
641 Wachenfeld DR, Willis BL, Wilson SK (2017) Global warming and recurrent mass bleaching of
642 corals. *Nature* 543:373–377 . <https://doi.org/10.1038/nature21707>
- 643 Hulbert SH (1984) Pseudoreplication and the Design of Ecological Field Experiments. *Ecol Monogr*
644 54:187–211
- 645 Işkın U, Filiz N, Cao Y, Neif ÉM, Öglü B, Lauridsen TL, Davidson TA, Søndergaard M, Tavşanoğlu
646 ÜN, Beklioğlu M, Jeppesen E (2020) Impact of nutrients, temperatures, and a heat wave on
647 zooplankton community structure: An experimental approach. *Water (Switzerland)* 12:1–19 .
648 <https://doi.org/10.3390/w12123416>
- 649 Jiménez-Quiroz M del C, Cervantes-Duarte R, Funes-Rodríguez R, Barón-Campis SA, García-
650 Romero F de J, Hernández-Trujillo S, Hernández-Becerril DU, González-Armas R, Martell-
651 Dubois R, Cerdeira-Estrada S, Fernández-Méndez JI, González-Ania L V., Vásquez-Ortiz M,
652 Barrón-Barraza FJ (2019) Impact of “The Blob” and “El Niño” in the SW Baja California
653 Peninsula: Plankton and environmental variability of Bahía Magdalena. *Front Mar Sci* 6:1–23 .
654 <https://doi.org/10.3389/fmars.2019.00025>
- 655 Jokiel PL, Coles SL (1990) Response of Hawaiian and other Indo-Pacific reef corals to elevated
656 temperature. *Coral Reefs* 8:155–162 . <https://doi.org/10.1007/BF00265006>
- 657 Jones T, Parrish JK, Peterson WT, Bjorkstedt EP, Bond NA, Ballance LT, Bowes V, Hipfner JM,
658 Burgess HK, Dolliver JE, Lindquist K, Lindsey J, Nevins HM, Robertson RR, Roletto J, Wilson
659 L, Joyce T, Harvey J (2018) Massive Mortality of a Planktivorous Seabird in Response to a
660 Marine Heatwave. *Geophys Res Lett* 45:3193–3202 . <https://doi.org/10.1002/2017GL076164>
- 661 Kim SW, Sampayo EM, Sommer B, Sims CA, Gómez-Cabrera M del C, Dalton SJ, Beger M,
662 Malcolm HA, Ferrari R, Fraser N, Figueira WF, Smith SDA, Heron SF, Baird AH, Byrne M,
663 Eakin CM, Edgar R, Hughes TP, Kyriacou N, Liu G, Matis PA, Skirving WJ, Pandolfi JM
664 (2019) Refugia under threat: mass bleaching of coral assemblages in high-latitude eastern
665 Australia. *Glob Chang Biol* 00:1–14 . <https://doi.org/10.1111/gcb.14772>
- 666 Kirk NL, Howells EJ, Abrego D, Burt JA, Meyer E (2018) Genomic and transcriptomic signals of
667 thermal tolerance in heat-tolerant corals (*Platygyra daedalea*) of the Arabian/Persian Gulf. *Mol*
668 *Ecol* 27:5180–5194 . <https://doi.org/10.1111/mec.14934>
- 669 LaJeunesse TC, Parkinson JE, Gabrielson PW, Jeong HJ, Reimer JD, Voolstra CR, Santos SR (2018)
670 Systematic Revision of Symbiodiniaceae Highlights the Antiquity and Diversity of Coral
671 Endosymbionts. *Curr Biol* 28:2570-2580.e6 . <https://doi.org/10.1016/j.cub.2018.07.008>
- 672 Liew YJ, Howells EJ, Wang X, Michell CT, Burt JA, Idaghdour Y, Aranda M (2020)
673 Intergenerational epigenetic inheritance in reef-building corals. *Nat Clim Chang* 10:254–259 .
674 <https://doi.org/10.1038/s41558-019-0687-2>
- 675 Little RJ, Rubin DB (2002) *Statistical analysis with missing data*. John Wiley & Sons, Ltd
- 676 Liu G, Heron SF, Mark Eakin C, Muller-Karger FE, Vega-Rodriguez M, Guild LS, de la Cour JL,
677 Geiger EF, Skirving WJ, Burgess TFR, Strong AE, Harris A, Maturi E, Ignatov A, Sapper J, Li
678 J, Lynds S (2014) Reef-scale thermal stress monitoring of coral ecosystems: New 5-km global
679 products from NOAA coral reef watch. *Remote Sens* 6:11579–11606 .
680 <https://doi.org/10.3390/rs61111579>
- 681 Liu G, Rauenzahn J, Heron S, Eakin C, Skirving W, Christensen T, Strong A, Li J (2013) NOAA

- 682 Coral Reef Watch 50 km Satellite Sea Surface Temperature-Based Decision Support System for
683 Coral Bleaching Management
- 684 Liu G, Strong AE, Skirving W (2003) Remote sensing of sea surface temperatures during 2002 barrier
685 reef coral bleaching. *Eos (Washington DC)* 84:2002–2004 .
686 <https://doi.org/10.1029/2003EO150001>
- 687 Marshall PA, Baird AH (2000) Bleaching of corals on the Great Barrier Reef: Differential
688 susceptibilities among taxa. *Coral Reefs* 19:155–163 . <https://doi.org/10.1007/s003380000086>
- 689 Matz M V., Treml EA, Aglyamova G V., Bay LK (2018) Potential and limits for rapid genetic
690 adaptation to warming in a Great Barrier Reef coral. *PLoS Genet* 14:1–19 .
691 <https://doi.org/10.1371/journal.pgen.1007220>
- 692 McClanahan TR, Darling ES, Maina JM, Muthiga NA, D’Agata S, Leblond J, Arthur R, Jupiter SD,
693 Wilson SK, Mangubhai S, Ussi AM, Guillaume MMM, Humphries AT, Patankar V, Shedrawi
694 G, Pagu J, Grimsditch G (2020) Highly variable taxa-specific coral bleaching responses to
695 thermal stresses. *Mar Ecol Prog Ser* 648:135–151 . <https://doi.org/10.3354/meps13402>
- 696 Mumby PJ, Chisholm JRM, Edwards AJ, Andrefouet S, Jaubert J (2001) Cloudy weather may have
697 saved Society Island reef corals during the 1998 ENSO event. *Mar Ecol Prog Ser* 222:209–216 .
698 <https://doi.org/10.3354/meps222209>
- 699 Nakagawa S, Freckleton RP (2008) Missing inaction: the dangers of ignoring missing data. *Trends*
700 *Ecol Evol* 23:592–596 . <https://doi.org/10.1016/j.tree.2008.06.014>
- 701 Oliver ECJ, Donat MG, Burrows MT, Moore PJ, Smale DA, Alexander L V., Benthuyzen JA, Feng
702 M, Sen Gupta A, Hobday AJ, Holbrook NJ, Perkins-Kirkpatrick SE, Scannell HA, Straub SC,
703 Wernberg T (2018) Longer and more frequent marine heatwaves over the past century. *Nat*
704 *Commun* 9:1–12 . <https://doi.org/10.1038/s41467-018-03732-9>
- 705 Piatt JF, Parrish JK, Renner HM, Schoen SK, Jones TT, Arimitsu ML, Kuletz KJ, Bodenstern B,
706 García-Reyes M, Duerr RS, Corcoran RM, Kaler RSA, McChesney GJ, Golightly RT, Coletti
707 HA, Suryan RM, Burgess HK, Lindsey J, Lindquist K, Warzybok PM, Jahncke J, Roletto J,
708 Sydeman WJ (2020) Extreme mortality and reproductive failure of common murrelets resulting
709 from the northeast Pacific marine heatwave of 2014–2016
- 710 Robin X, Turck N, Hainard A, Tiberti N, Lisacek F, Sanchez J-C, Müller M (2011) pROC: an open-
711 source package for R and S+ to analyze and compare ROC curves. *BMC Bioinformatics* 12: .
712 <https://doi.org/10.1186/147121051277>
- 713 Romero-Torres M, Acosta A, Palacio-Castro AM, Treml EA, Zapata FA, Paz-García DA, Porter JW
714 (2020) Coral reef resilience to thermal stress in the Eastern Tropical Pacific. *Glob Chang Biol*
715 26:3880–3890 . <https://doi.org/10.1111/gcb.15126>
- 716 Rue H, Martino S, Chopin N (2009) Approximate Bayesian inference for latent Gaussian models by
717 using integrated nested Laplace approximations. *J R Stat Soc Ser B Stat Methodol* 71:319–392 .
718 <https://doi.org/10.1111/j.1467-9868.2008.00700.x>
- 719 Safaie A, Silbiger NJ, McClanahan TR, Pawlak G, Barshis DJ, Hench JL, Rogers JS, Williams GJ,
720 Davis KA (2018) High frequency temperature variability reduces the risk of coral bleaching. *Nat*
721 *Commun* 9:1–12 . <https://doi.org/10.1038/s41467-018-04074-2>
- 722 Skirving W, Enríquez S, Hedley JD, Dove S, Eakin CM, Mason RAB, Cour JLD La, Liu G, Hoegh-
723 Guldborg O, Strong AE, Mumby PJ, Iglesias-Prieto R (2018) Remote sensing of coral bleaching
724 using temperature and light: Progress towards an operational algorithm. *Remote Sens* 10: .
725 <https://doi.org/10.3390/rs10010018>
- 726 Skirving W, Marsh B, De La Cour J, Liu G, Harris A, Maturi E, Geiger E, Mark Eakin C (2020)
727 Coraltemp and the coral reef watch coral bleaching heat stress product suite version 3.1. *Remote*
728 *Sens* 12:1–10 . <https://doi.org/10.3390/rs12233856>
- 729 Skirving WJ, Heron SF, Marsh BL, Liu G, De La Cour JL, Geiger EF, Eakin CM (2019) The

- 730 relentless march of mass coral bleaching: a global perspective of changing heat stress. *Coral*
731 *Reefs* 38:547–557 . <https://doi.org/10.1007/s00338-019-01799-4>
- 732 Smale DA, Wernberg T, Oliver ECJ, Thomsen M, Harvey BP, Straub SC, Burrows MT, Alexander L
733 V., Benthuisen JA, Donat MG, Feng M, Hobday AJ, Holbrook NJ, Perkins-Kirkpatrick SE,
734 Scannell HA, Sen Gupta A, Payne BL, Moore PJ (2019) Marine heatwaves threaten global
735 biodiversity and the provision of ecosystem services. *Nat Clim Chang* 9:306–312 .
736 <https://doi.org/10.1038/s41558-019-0412-1>
- 737 Spady BL, Devotta DA, De La Cour J, Gomez AM, Morgan JA, Donner SD, Liu G, Skirving WJ,
738 Vasile R, Geiger E, Marsh B, Eakin CM, Manzello DP (2021) Global Coral Bleaching Database
739 (NCEI Accession 0228498). In: NOAA Natl. Centers Environ. Information. Unpubl. Dataset.
740 <https://www.ncei.noaa.gov/archive/accession/0228498>. Accessed 1 Sep 2020
- 741 Sully S, Burkepile DE, Donovan MK, Hodgson G, van Woesik R (2019) A global analysis of coral
742 bleaching over the past two decades. *Nat Commun* 10:1–5 . [https://doi.org/10.1038/s41467-019-](https://doi.org/10.1038/s41467-019-09238-2)
743 [09238-2](https://doi.org/10.1038/s41467-019-09238-2)
- 744 Ummenhofer CC, Meehl GA (2017) Extreme weather and climate events with ecological relevance:
745 A review. *Philos Trans R Soc B Biol Sci* 372: . <https://doi.org/10.1098/rstb.2016.0135>
- 746 Veron JEN (1995) *Corals in space and time: the biogeography and evolution of the Scleractinia*.
747 Cornell University Press
- 748 von Biela VR, Arimitsu ML, Piatt JF, Heflin BM, Schoen S (2019) Extreme reduction in condition of
749 a key forage fish during the Pacific marine heatwave of 2014–2016. *Mar Ecol Prog Ser*
750 613:171–182
- 751 Weeks SJ, Anthony KRN, Bakun A, Feldman GC, Hoegh-Guldberg O (2008) Improved predictions
752 of coral bleaching using seasonal baselines and higher spatial resolution. *Limnol Oceanogr*
753 53:1369–1375 . <https://doi.org/10.4319/lo.2008.53.4.1369>
- 754 Wellington GM, Glynn PW, Strong AE, Navarrete SA, Wieters E, Hubbard D (2001) Crisis on coral
755 reefs linked to climate change. *Eos (Washington DC)* 82:1–5 .
756 <https://doi.org/10.1029/01EO00001>
- 757 Wiedenmann J, D’Angelo C, Smith EG, Hunt AN, Legiret FE, Postle AD, Achterberg EP (2013)
758 Nutrient enrichment can increase the susceptibility of reef corals to bleaching. *Nat Clim Chang*
759 3:160–164 . <https://doi.org/10.1038/nclimate1661>
- 760 Wyatt ASJ, Leichter JJ, Toth LT, Miyajima T, Aronson RB, Nagata T (2019) Heat accumulation on
761 coral reefs mitigated by internal waves. *Nat Geosci*. <https://doi.org/10.1038/s41561-019-0486-4>
- 762 Wyatt ASJ, Leichter JJ, Toth LT, Miyajima T, Aronson RB, Nagata T (2020) Heat accumulation on
763 coral reefs mitigated by internal waves. *Nat Geosci* 13:28–34 . [https://doi.org/10.1038/s41561-](https://doi.org/10.1038/s41561-019-0486-4)
764 [019-0486-4](https://doi.org/10.1038/s41561-019-0486-4)
- 765 Zuur AF, Ieno EN (2017) *Beginner’s Guide to Spatial, Temporal and Spatial-Temporal Ecological*
766 *Data Analysis with R-INLA. Volume II GAM and Zero-Inflated Models*. Highland Statistics
767 Ltd, 1
- 768
- 769